e-ISSN: 2980-0463
Anat. J. Pharm. Sci., 2024:3(1)
AJPS
Research Article

Investigation of the Adsorption of 6-(3-(4-(2-methoxyphenyl)piperazin-1-yl)propylamino)-1,3-dimethylpyrimidine-2,4(1*H*,3*H*)-dione (urapidil) on Graphene Oxide by Density Functional Theory Calculation Method

Begum Cagla AKBAS[1], Mehmet Abdullah ALAGOZ[1], Esvet AKBAS[2*]

[1] Faculty of Pharmacy, Inonu University, Malatya, Türkiye

[2] Department of Chemistry, Faculty of Science, Van Yuzuncu Yil University, Van, Türkiye

ABSTRACT: Graphene oxide (GO) has become a very interesting structure in recent years due to its important results in biomedical applications of nano-bio researchers. Graphene oxide is a form of graphene decorated with oxygen-containing groups. When compared to graphene, GO is easily dispersible in water as well as any other solvents. It is easy to process and also make graphene too. Graphene-based materials are also widely used studied in biomedical applications in smart medicine and genetic engineering. In this work, the electronic properties of commercially available pyrimidine-2,4(1*H*,3*H*)-dione used in antihypertensive treatment and its adsorption on GO nanocage were calculated using density functional theory (DFT). Based on calculations, it is probable that the urapidil molecule's -NH group will interact with the GO surface's acid group. Most likely, proton exchange is the basis for the adsorption taking place in this section. The N-O interaction bond length was found to be 2.05115A° in the computation done within the context of this option.

Keywords: *urapidil, ebrantil, graphene oxide, antihypertensive*

1 INTRODUCTION

GO was synthesized by oxidation of graphite to graphite oxide followed by exfoliation [1]. GO has a large surface area and contains many epoxy and hydroxyl groups on its surface [2-6]. GO are important for material science because of thermal, optical, electrical and magnetic properties [7-9]. GO chemistry is largely based on Brodie's work on graphite oxide in the 18th century [10]. Generally accepted models of GO structure are those based on hydroxyl, carboxylic acid and epoxide groups as the dominant functional groups (Figure 1). It also contains groups such as ketones, phenols, lactols and lactones in its structure [11]. There are many outstanding properties that define such materials in terms of reactivity. Oxygen-containing functional groups cause GO to function as a solid acid. The nanovoids present in GO give it unpaired spins, which helps in the activation of small molecules by the spin flip process. GO is an ideal material where covalent modification or non-covalent interactions occur [12]. Figure 1 shows potential active sites that can be added to the GO scaffold. The bonding between GO and organic materials can be covalent bond or

*Corresponding Author: Esvet AKBAS
E-mail: esvakbas@hotmail.com
Submitted: 14.12.2023 Accepted: 19.02.2024

non-covalent bond interaction. GO has been extensively researched to develop biosensors due to its functionalizable surface and sensitive electrical properties [13, 14]. Detection of important biomolecules such as nucleic acids, proteins, and growth factors has been successfully achieved using appropriately functionalized graphene derivatives [15]. In addition to biomolecules in buffered solutions, hormonal catechol amine molecules secreted from living neuroendocrine cells have been also detected using GO [16].

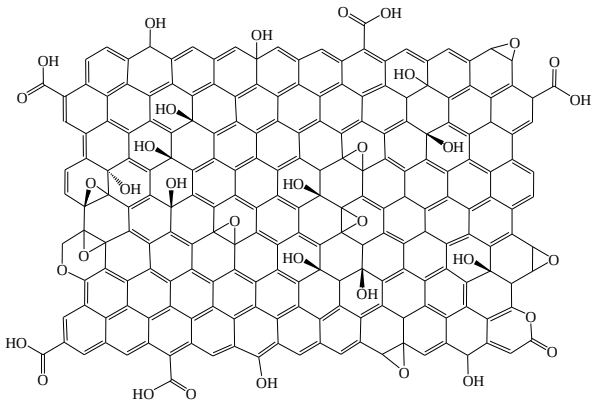

Figure 1. Proposed structure of GO [17].

Single malaria-infected red blood cells have also been detected by devices fabricated on microfluidic channel arrays and graphene films functionalized with receptor proteins [18].

Patients with hypertension are at an increased risk of morbidity and mortality from cardiovascular diseases (stroke and coronary events). The magnitude of this risk depends on the severity of hypertension. The goal of treatment is to lower blood pressure, thereby reducing the risk of stroke and coronary events. Drugs commonly used to treat hypertension include diuretics, β-receptor blocking drugs, angiotensin-converting enzyme (ACE) inhibitors, calcium antagonists, and α-adrenoceptor antagonists [19]. This pyrimidine derivative (Figure 2) is a widely used drug with antihypertensive effects in central and peripheral areas. This compound blocks the effects of the nervous system on the vascular muscular system.

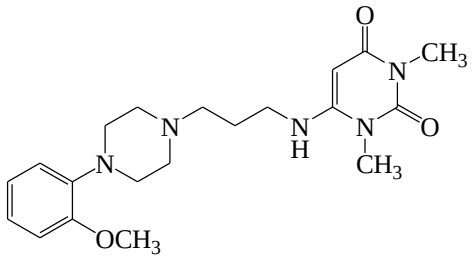

Figure 2. Pyrimidine derivative.

Quantum chemistry methods play an important role in obtaining extremely precise geometries for molecules and predicting various properties of molecules. Density functional theory (DFT) methods offer an alternative use of inexpensive computational methods in studying the properties of relatively large molecules [20]. DFT is widely used to study the electronic properties, molecular structure, chemical reactivity and hydrogen bonding of pharmaceutical compounds [21]. With DFT calculations, the

molecular orbitals and geometries of organic compounds are characterized by their activities. The properties of the components are related to the highest occupied molecular orbital energy (E_{HOMO}), the lowest unoccupied molecular orbital energy (E_{LUMO}) and the use of frontier orbital energy difference ($\Delta E = E_{LUMO} - E_{HOMO}$) [22]. In this study, the geometric and electronic structures of the 6-(3-(4-(2-methoxyphenyl) piperazin -1-yl)propylamino) -1,3- dimethylpyrimidine-2,4 (1*H*,3*H*) -dione (urapidil) , used as an antihypertensive drug, were examined by the DFT method. The adsorption of compound on graphene oxide was studied with the same method.

2 MATERIAL AND METHOD

2.1 Materials

The adsorption of urapidil molecule on the GO nanocage surface was investigated by DFT calculations. The calculations are made on Gaussian09 program using the B3LYP/DGTZVP basis set [23-25]. To accurately the interaction, the adsorption energies (ΔEad) were calculated as follows:

$$\Delta Ead = \Delta E(complex) - \Delta E(GO) - \Delta E(pyrimidine\ derivative) \quad (1)$$

Quantum chemical parameters ΔE_{HOMO}, ΔE_{LUMO} and ΔE_{gap} were calculated and discussed for all types of interactions.

In addition, electronegativity "χ", chemical softness "S", ionization potential "I", dipole moment "μ", chemical hardness "η" and electron affinity "A" [26, 27] calculations were performed for GO and pyrimidine derivative.

3 RESULTS AND DISCUSSION

Full geometry optimizations of the GO nanocage and urapidil were performed using DFT based on Beck and Lee–Yang–Parr [28] non-local correlation functional (B3LYP) DGTZVP basis sets in the Gaussian09 program [23] (Fig. 3a,b).

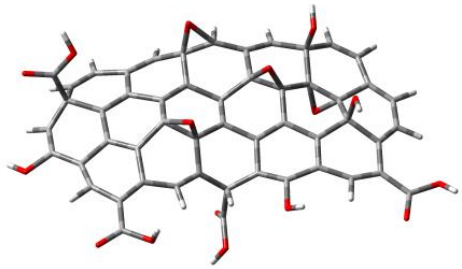

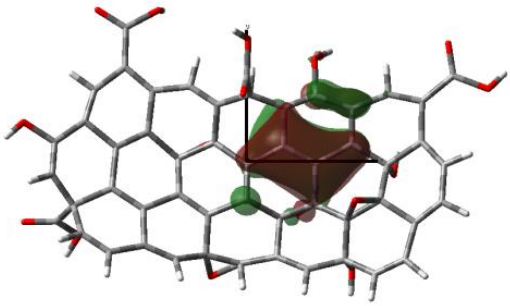

HOMO

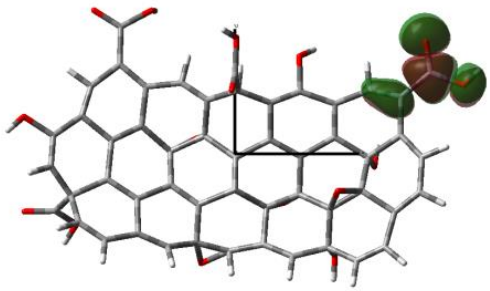

LUMO

Figure 3a. GO nanocage HOMO and LUMO profile.

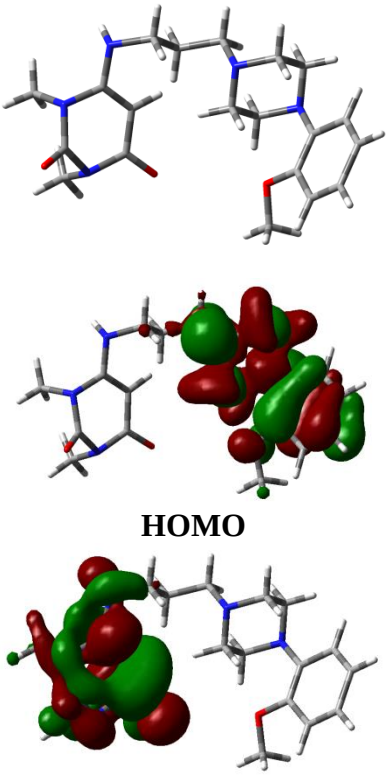

Figure 3b. Pyrimidine derivative HOMO and LUMO profile.

When the electronic structure of the GO nanocage is examined, it is seen that electrons are concentrated in the epoxy regions. It is seen that the electrophilic character is concentrated in the carboxylic acid regions. This shows that the aliphatic nitrogen atom on the pyrimidine derivative will attach to the carboxylic acid region of GO. The adsorption of pyrimidine derivative on the GO surface can be analyzed by theoretical calculations. HOMO and LUMO values are the most important parameters used to predict the adsorption activity of pyrimidine derivative on the GO surface. In addition, parameters such as ionization potential, electron affinity, chemical softness, dipole moment, chemical hardness and electronegativity can be obtained through quantum calculations.

The absolute electronegativity (χ) of the compounds is calculated with the following equation (2), depending on the ionization potential and electron affinity [29].

$$\chi = \left(\frac{I+A}{2}\right) \qquad (2)$$

The chemical hardness of the compound is calculated based on its ionization potential and electron affinity (equality) (3).

$$\eta = \frac{1}{2}\left(\frac{\partial^2 E}{\partial N^2}\right)_{\vartheta(r)} = \frac{1}{2}\left(\frac{\partial \mu}{\partial N}\right) = \frac{I-A}{2} \qquad (3)$$

Another important parameter that shows the reactivity of compounds is chemical softness. Chemical hardness and softness are also connected to each other as in the equation below.

$$S = \frac{1}{\eta} \qquad (4)$$

Obtained HOMO, LUMO, I, A, χ, η and S values as a result of the calculations are given in table 1.

Table 1. The quantum chemical parameters for GO and pyrimidine derivative (e*V*).

	E_{HOMO}	E_{LUMO}	ΔE	I	A
GO	-7.169	-0.975	6.194	7.169	0.975
Ura	-4.941	-1.899	3.042	4.941	1.899
	η	S	χ	*μ(D)*	
GO	6.194	0.161	4.072	6.472	
Ura	1.521	0.657	3.420	4.923	

Nonlinear optical properties for GO and pyrimidine derivative were calculated. As a result of these calculations, total dipole moment μ_{tot}, average polarizability (α_{tot}) and average first hyperpolarizability (β_{tot}) were calculated.

$$\mu tot = \mu_X^2 + \mu_Y^2 + \mu_Z^2 \quad (5)$$

$$\alpha tot = (\alpha_{xx} + \alpha_{yy} + \alpha_{zz})/3 \quad (6)$$

$$\beta tot = [(\beta_{xxx} + \beta_{xyy} + \beta_{xzz})^2 + (\beta_{yxx} + \beta_{yxx} + \beta_{yzz})^2 + (\beta_{zzz} + \beta_{zxx} + \beta_{zyy})^2]^{\frac{1}{2}} \quad (7)$$

The values of the resulting calculations are given in Table 2. The high dipole moment, molecular polarizability and hyper polarizability values of the compound are directly proportional to its good nonlinear optical (NLO) properties. According to the values obtained as a result of the calculations, it was determined that the compounds studied had very good NLO properties.

The molecular electrostatic potential maps (MEPs) were calculated using DFT and DGTZVP base set in the Gaussian09 program for GO and pyrimidine derivative. In MEPs, which provide important information about the charge distribution of the molecules, the charge distributions are given in different colors. In the MEPs given in Figure 4a,b the areas represented in red represent the regions where negativity is concentrated in the molecule (nucleophile), and the regions in blue color represent the areas in the molecule where positivity is concentrated (electrophile). The electrostatic potential increases during red> orange> yellow> green> blue. In these our compounds the highest potential is on oxygen atoms.

Table 2. NLO properties of GO, pyrimidine derivative and complex structure.

Parameters (a.u)	GO	pyrimidine derivative	Complex
β_{xxx}	589.8926	-105.3978	-803.5864
β_{xyy}	155.7559	32.8724	-144.4748
β_{xzz}	-60.7116	24.9881	-32.0193
β_{yyy}	-269.3956	2.4770	1059.2316
β_{yxx}	-228.1507	36.0261	136.2827
β_{yzz}	78.0111	-7.3493	16.9900
β_{zzz}	-51.6876	-18.0063	-36.8272
β_{xxz}	69.4933	-56.0057	256.9811
β_{zyy}	7.4148	-26.0346	168.5767
β_{tot} (esu) 10^{-33}	803.607	115.0637	1606,79
α_{xx}	17.9609	-153.5790	-441.7985
α_{yy}	-1.5240	-156.9748	-553.2645
α_{zz}	-16.4370	-180.6349	-577.7118
α_{tot} (esu) 10^{-33}	-0.00003	-163.7296	-524.2582
μ_x	4.3060	-0.7441	-9.8410
μ_y	-4.6709	3.5837	8.2756
μ_z	1.2362	-3.2930	5.0619
μ_{tot} (esu) 10^{-33}	6.4720	4.9234	13.8186

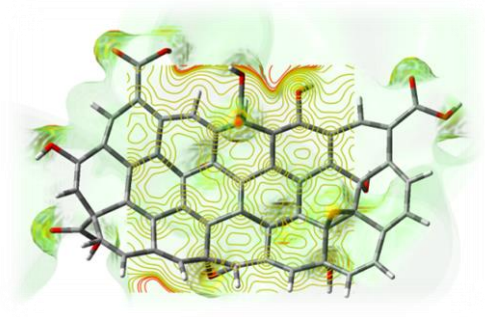

Figure 4a. MEP of GO.

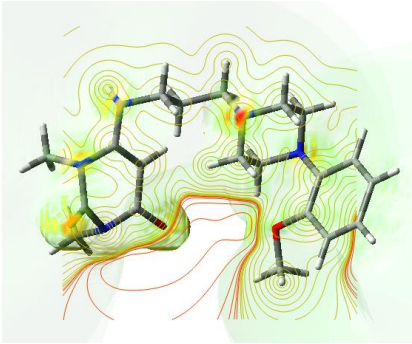

Figure 4b. MEP of pyrimidine derivative.

Calculations show that the -NH group in the pyrimidine derivative is likely to interact with the acid group on the GO surface. The adsorption occurring in this part is most likely based on proton exchange. In the calculation made within the framework of this possibility, it was determined that the N-O interaction bond length was 2.0511A^0 (Figure 5).

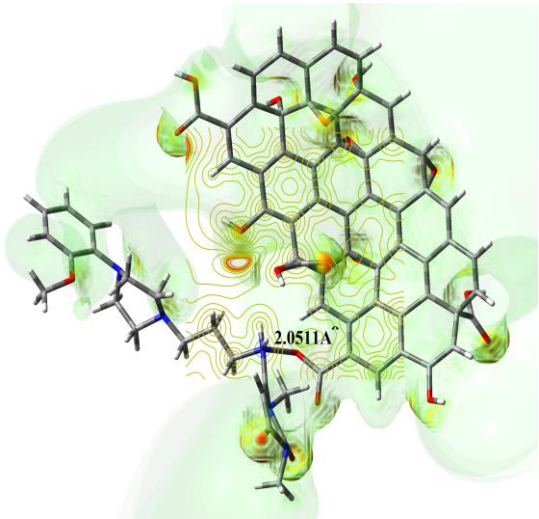

Figure 5. Complex of pyrimidine derivative/GO.

The electronic energy of the pyrimidine derivative /GO complex was calculated by the following equation.

$$\Delta Ead = \Delta E(complex) - \Delta E(GO) - \Delta E(pyrimidine\ derivative)$$

$$\Delta Ead = (-164{,}50) - \Delta E(-117{,}49) - \Delta E(-46{,}99)$$

$$\Delta Ead = -0.02\ eV$$

Accordingly, the two main mechanisms involved in the adsorption of pyrimidine derivative to the carboxylic acid site on the GO nanocage surface are orbital and charge-induced interactions (electrostatic effect). In particular, the hydrogen atom bonded to the nitrogen atom interacts with the oxygen in the carboxylic acid group, inducing intermolecular electrostatic interactions. Consequently, complex is the most stable from its NH side due to the interaction between pyrimidine derivative and the GO nanocage.

Figure 6 shows the density of the state spectra for pyrimidine derivative and complex. The decrease in the Eg value of the GO- pyrimidine derivative compared to the GO nanocage is due to this opposite electric peak after the adsorption process of pyrimidine derivative. Furthermore, a closer examination of the DOS spectrum reveals that the HOMO and especially the LUMO levels are shifted to the higher energy region after adsorption of pyrimidine derivative.

Based on the computation findings, it is possible to conclude that the pyrimidine derivative molecule's -NH group will create a strong bond through proton transfer with the

acid group on the GO surface during adsorption.

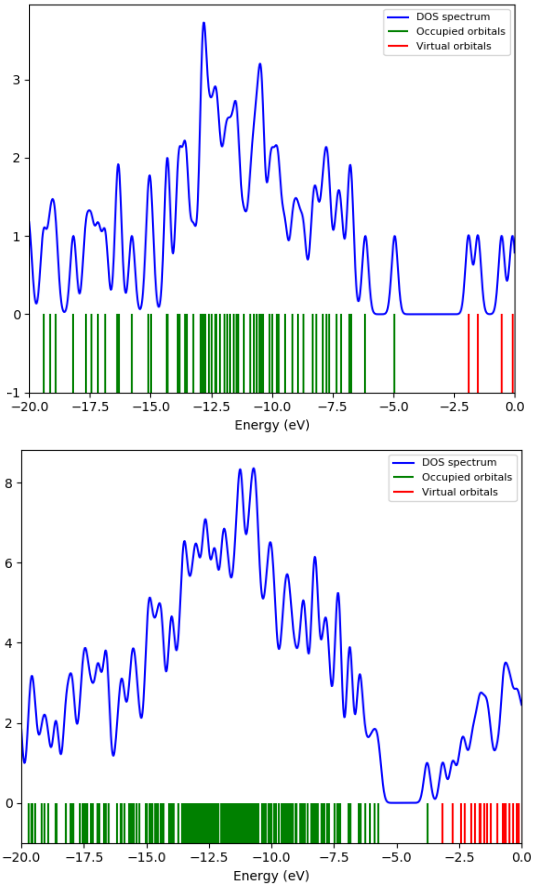

Figure 6. DOS plots of pristine pyrimidine derivative and complex, respectively.

4 ACKNOWLEDGEMENTS

This work was supported by TUBİTAK-BİDEB-2209/2-1919B012005277

5 CONFLICT OF INTEREST

Authors declare that there is no a conflict of interest with any person, institute, company, etc.

6 REFERENCES

[1] Krishnamoorthy K, Kim G.S, Kim S.J. Graphene nanosheets: Ultrasound assisted synthesis and Characterization, Ultrason Sonochem., 2013; 20, 644–649.

[2] Mouhat F, Coudert F. X, Bocquet L. M. Structure and chemistry of graphene oxide in liquid water from first principles, Nature Communications, 2020, 11(1)1566.

[3] Valentini L, Bittolo Bon S, Giorgi G. Engineering Graphene Oxide/Water Interface from First Principles to Experiments for Electrostatic Protective Composites, Polymers (Basel), 2020, 12, (7) 1596.

[4] Ramesha G.K, Kumara A.V, Muralidhara H.B, Sampath S. Graphene and graphene oxide as effective adsorbents toward anionic and cationic dyes, J. Colloid Interface Sci. 2011, 361, 270–277.

[5] Zhu J, Wei S, Gu H, Rapole S.B, Wang Q, Luo Z, Haldolaarachchige N, Young D.P, Guo Z. One-Pot Synthesis of Magnetic Graphene Nanocomposites Decorated with Core@Double-shell Nanoparticles for Fast Chromium Removal, Environ. Sci. Technol. 2012, 46, (2) 977–985.

[6] Tiwari J.N, Mahesh K, Le N.H, Timilsina K.C.K.R, Tiwari R.N, Kim K.S. Understanding the adsorption property of graphene-oxide with different degrees of oxidation levels, Carbon, 2013, 56, 173–182.

[7] Bai J, Zhong X, Jiang S, Huang Y, Duan

X. Graphene nanomesh, Nat Mater., 2010, 5, 190–194.

[8] Li Z, Fan J, Tong C, et al. A smart drug-delivery nanosystem based on carboxylated graphene quantum dots for tumor-targeted chemotherapy, Nanomedicine, 2019, 14(15) 2011–2025.

[9] Fedotova A. K, Prischepa S. L, Fedotova J, et al., Electrical conductivity and magnetoresistance in twisted graphene electrochemically decorated with Co particles, Physica E: Low-dimensional Systems and Nanostructures, 2020, 117 113790.

[10] Brodie B. C. On the Atomic Weight of Graphite, Philos.Trans.R.Soc.London, 1859, 149, 249–259.

[11] Erickson K, Erni R, Lee Z, Alem N, Gannett W, Zettl A. Determination of the Local Chemical Structure of Graphene Oxide and Reduced Graphene Oxide, Adv. Mater, 2010, 22, 4467–4472.

[12] Loh K. P, Bao Q. L, Ang P. K, Yang J. X. The Chemistry of Graphene, J. Mater. Chem., 2010, 20, 2277–2289

[13] Mohanty N, Berry V. Graphene-based single-bacterium resolution biodevice and DNAtransistor: interfacing graphene derivatives with nanoscale and microscale biocomponents, .Nano Lett. 2008, 8, 4469–4476.17

[14] Ohno Y, Maehashi K, Matsumoto K. Label-free biosensors based on aptamer-modifiedgraphene field-effect transistors, J. Am. Chem. Soc. 2010,132, 18012–18013

[15] Kwon O.S, Park S.J, Hong J.Y, Han A.R, Lee J.S, Lee J.S, Oh J.H, Jang J. Flexible FET-type VEGF aptasensor based on nitrogen-doped graphene converted from conducting polymer, ACS Nano, 2012, 6, 1486–1493

[16] He Q, Sudibya H. G, Yin Z, Wu S, Li H, Boey F, Huang W, Chen P, Zhang H. Centimeter-long and large-scale micropatterns of reduced graphene oxide films: fabricationand sensing applications, ACS Nano, 2010, 4, 3201–3208.

[17] Georgakilas V, Tiwari J. N, Kemp K. C, Perman J. A, Bourlinos A. B, Kim K. S, and Zboril R. Noncovalent Functionalization of Graphene and Graphene Oxide for Energy Materials, Biosensing, Catalytic, and Biomedical Applications, Chem. Rev. 2016, 116, 9, 5464–5519.

[18] Ang P. K, Li A, Jaiswal M, Wang Y, Hou H. W, Thong J. T, Lim C. T, Loh K. P. Flowsensing of single cell by graphene transistor in a microfluidic channel, Nano Lett., 2011,11,5240–5246.

[19] Dooley M, Goa, K.L. Urapidil A Reappraisal of its Use in the Management of Hypertension, Adis Drug Evaluation, 1998, 56 (5): 929-55.

[20] Davidson E. R. Quantum Theory of Matter: Introduction, Chemical Reviews, 1991, 91 (5):649.

[21] Palafox M.A, Rastogi V.K, Tanwar R.P, Mittal L. Vibrational frequencies and structure of 2-thiouracil by Hartree-Fock, post-Hartree-Fock and density functional methods, Spectrochim. Acta - Part A Mol. Biomol. Spectrosc., 2003, 59:2473–86.

[22] Kanmazalp S.D. Investigation of Theoretical Calculations of 2-(1-Phenylethylideneamino)guanidine Compound: NBO, NLO, HOMO-LUMO and MEP Analysis by DFT Method, Karaelmas Fen ve Mühendislik Dergisi, 2017, 7(2), 491-496.

[23] Frisch M. J, Trucks G. W, Schlegel H. B, Scuseria G. E, Robb M. A, Cheeseman J. R, Scalmani G, Barone V, Mennucci B, Petersson G. A, H Nakatsuji, Caricato M, Li X, Hratchian H. P, Izmaylov A. F, Bloino J, Zheng G, Sonnenberg J. L, Hada M, Ehara M, Toyota K, Fukuda R, Hasegawa J, Ishida M, Nakajima T, Honda Y, Kitao O, Nakai H, Vreven T, Montgomery J. A, Peralta Jr. J. E, Ogliaro F, Bearpark M, Heyd J. J, Brothers E, Kudin K. N, Staroverov V. N, Kobayashi R, Normand J, Raghavachari K, Rendell A, Burant J. C, Iyengar S. S, Tomasi J, Cossi M, Rega N, Millam J. M, Klene M, Knox J. E, Cross J. B, Bakken V, Adamo C, Jaramillo J, Gomperts R, Stratmann R. E, Yazyev O, Austin A. J, Cammi R, Pomelli C, Ochterski J. W, Martin R. L, Morokuma K, Zakrzewski V. G, Voth G. A, Salvador P, Dannenberg J. J, Dapprich S, Daniels A. D, Farkas Ö, Foresman J. B, Ortiz J. V, Cioslowski J. and Fox D. J. Gaussian, Inc., Wallingford, 2009,CT, USA.

[24] Perdew J. P, Wang Y. Accurate and simple analytic representation of the electron-gas correlation energy, Phys. Rev. B. Condens. Matter; 1992, 45 13244–13249.

[25] Simos T. E, Tsitouras C, Kovalnogov V. N, Fedorov R. V, Generalov D. A. Real-Time Estimation of R0 for COVID-19 Spread, Mathematics (Basel), 2021, 9 664.

[26] Karzazi Y, Belghiti M.E. A, Dafali A, and Hammouti B. A theoretical investigation on the corrosion inhibition of mild steel by piperidine derivatives in hydrochloric acid solution, Journal of Chemical and Pharmaceutical Research, 2014, 6(4) 689-696.

[27] Glendening E. D, Landis C. R, Weinhold F. Natural bond orbital methods, WIREs Computational Molecular Science, 2011, 2, 1–42.

[28] Lee C, Yang W, Parr R. G. Development of the Colle-Salvetti correlation-energy formula into a functional of the electron density, Phys. Rev. B. 1988, 37, 785.

[29] Fleming I, Frontier Orbitals and Organic Chemical Reactions, John Wiley and Sons, New York,. 1976.